JOURNAL OF
Materials
CHEMISTRY

Aragonite crystals with unconventional morphologies

Debojit Chakrabarty and Samiran Mahapatra*

Unilever Research India, I.C.T Link Road, Chakala, Andheri (East), Mumbai, 400 099, India

Received 5th July 1999, Accepted 10th September 1999

Conventionally, the aragonite polymorph of $CaCO_3$ possesses a 'needle-like' morphology. Aragonite crystals with unconventional morphologies, like 'cauliflower' and 'flake', have been synthesised by combining aqueous solutions of $CaCl_2$ and Na_2CO_3 under ambient reaction conditions. The unambiguous characterisation of these aragonite polymorphs is based on their characteristic powder X-ray diffraction patterns, Raman and FTIR spectra. The morphologies of these aragonite crystals have been confirmed by scanning electron microscopy. Both 'cauliflower' and 'flake-like' aragonites are spectroscopically similar to their needle-like congener, except that they are less crystalline in nature and they exhibit minor differences in their FTIR spectra. A plausible mechanism for the formation of these aragonites has been proposed based on the phase transformation behaviour during their syntheses.

Introduction

The control of the crystal shape/morphology of calcium carbonate is important to its industrial uses as pigments, fillers and dentifrices, and of its biological role as structural supports in skeletons.[1–8] Pure calcium carbonate is polymorphous and occurs naturally in three anhydrous crystalline forms, *viz.* calcite, aragonite and vaterite. Amorphous calcium carbonate is also known in biological systems.[9] There are two further forms, namely calcite II and calcite III, which are known to occur only at high pressures.[10] Calcite is the thermodynamically most stable form of calcium carbonate at room temperature and at atmospheric pressure. In comparison, aragonite is slightly less stable under similar conditions and is eventually transformed to calcite.[11] However, the occurrence of both calcite and aragonite is very common and widespread in biologically produced calcium carbonate minerals.[1–7,11]

The conventional morphologies of calcite, aragonite and vaterite are rhombohedral, needle-like and spheroidal, respectively. The basic differences amongst these phases lie in the disposition of the carbonate ion with respect to the central Ca^{2+} ion in their respective unit cells. The spatial arrangement of Ca^{2+} ions is very similar in the (001) planes of both calcite and aragonite, and in both structures the carbonate ions lie with their molecular plane parallel to the *ab* layer. However, vaterite differs significantly from the other two, in that the planes of the $CO_3{}^{2-}$ ions are perpendicular to the Ca^{2+} ion planes. Although many studies have shown that a wide range of additives can influence the shape of calcite crystals grown under laboratory conditions, examples of morphological modification of non-biogenically prepared aragonites are rare.[12–24]

Two basic synthetic routes to prepare calcium carbonate are (i) the solution route,[25] wherein aqueous $CaCl_2$ and Na_2CO_3 are combined in an equimolar ratio [double decomposition reaction; eqn. (1)] and (ii) the carbonation route,[26] in which CO_2 gas is bubbled through an aqueous slurry of $Ca(OH)_2$ [eqn. (2)]. The latter also happens to be the industrial method of manufacture of precipitated $CaCO_3$.

$$CaCl_2 + Na_2CO_3 \rightarrow CaCO_3 + 2NaCl \qquad (1)$$

$$Ca(OH)_2 + CO_2 \rightarrow CaCO_3 + H_2O \qquad (2)$$

While the carbonation route leads to the isolation of pure calcite, it is difficult to obtain pure aragonite by this method. Calcite/aragonite intergrowth is almost always observed when carbonation is carried out in the temperature range 30–80 °C.[27] On the other hand, calcite, aragonite and vaterite can be obtained in their pure forms using the solution method of synthesis. Hence, we have chosen to make use of the solution method for the synthesis of aragonite samples in the present study.

While calcite is the main product obtained at room temperature, aragonite and vaterite formations are achieved at higher ($\sim$70 °C) and lower temperatures ($\sim$15 °C) respectively, using the solution method of preparation.[27] Aragonite synthesis under ambient conditions by the above route is not known to the best of our knowledge. However, it has been synthesised at room temperature using the Kitano method (from a supersaturated solution of calcium bicarbonate) in the presence of certain additives or beneath self-assembled monolayers.[12–23] Aragonites synthesised by all of the above methods exhibit their usual needle-like morphology. Here, we report facile synthetic methods by which specific morphological changes, hitherto unknown, can be induced in aragonite crystals. The preparation involves double decomposition of aqueous solutions of $CaCl_2$ and Na_2CO_3 at room temperature and, without the use of any additive or crystal habit modifier, leads to the formation of aragonites possessing unconventional morphologies, like 'cauliflower' and 'flake'. These aragonite samples are stable in their solid states for long times and, to the best of our knowledge, represent the first examples of its kind possessing such morphologies.

Experimental

$CaCl_2{\cdot}2H_2O$ (AR Grade) and Na_2CO_3 (anhydrous, AR Grade) were obtained from Loba Chemie (India) and were used as received. The syntheses of various calcium carbonate samples were conducted in a jacketed stainless steel reactor of internal working volume 20 L. The impeller speed for all experiments was maintained at 600 rpm. Water was circulated through the jacket during the course of the experiment to maintain a constant reaction temperature. A schematic outline of the reactor with relevant details is shown in Fig. 1.

Preparation of 'cauliflower-like' aragonite

Aqueous $CaCl_2$ (1 M, 735 g dissolved in 5 L H_2O) was added at a feed rate of 90 mL min^{-1} to an aqueous solution of Na_2CO_3 (1 M, 530 g dissolved in 5 L H_2O) whose temperature was maintained at 32 ± 1 °C. There was an initial reduction in the impeller speed because of the resistance offered by the thick

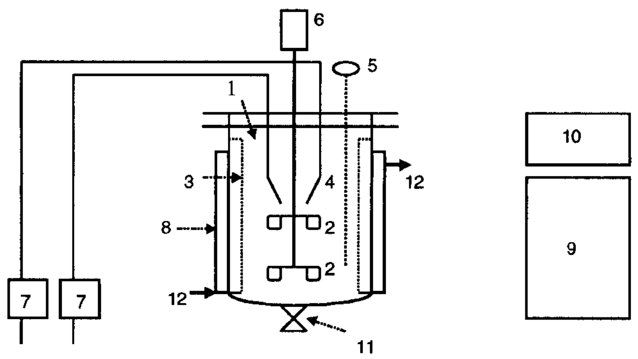

Fig. 1 A schematic outline of the reactor used for the synthesis of aragonite samples. Details of the reactor: (1) stirred tank reactor (internal diameter of 27 cm), (2) impeller consisting of flat blade turbine with four hub-mounted blades (two such impellers with diameter of 10 cm), (3) baffles (four), (4) feed lines entering near the eye of the impeller, (5) temperature indicator, (6) variable speed motor, (7) metering pumps for feeds, (8) jacket for cold/hot water, (9) constant temperature tank/circulator, (10) speed controller, (11) flush bottom valve and (12) inlet and outlet for water circulation.

gelatinous mass formed during the initial stages of the reaction. Subsequently, the gelation decreased and the calcium carbonate slurry was more amenable to stirring. After the completion of the reaction, the precipitate was filtered off, washed extensively with water and dried overnight at 110 °C. The dried cake was ground to a powder using a mixer. This material was obtained as a dense free-flowing white powder. Yield: 440 g (88%). Tapped bulk density (B.D.): 1.1 g cm^{-3}. Particle size distribution: d_{10}, 32.9; d_{50}, 42.8; d_{90}, 61.1 µm. BET Surface area: 7 m^2 g^{-1}. TGA (% weight loss): 43.78 (theor. value 43.96%).

Preparation of 'flake-like' aragonite

Aqueous Na_2CO_3 (2 M, 1.06 kg dissolved in 5 L H_2O) was stirred in the stainless steel reactor, the temperature of which was maintained at 25 °C. To this solution was then added aqueous $CaCl_2$ (2 M, 1.47 kg dissolved in 5 L H_2O) at a rate of 90 mL min^{-1} and the temperature was maintained at 25 °C until completion of reaction. In this case too, like the earlier example, the formation of a thick gelatinous mass during the initial stages of the reaction was noticed. At the end of the reaction, the precipitate was filtered off, washed extensively with water and dried overnight at 110 °C. The dried cake was ground to a powder using a mixer. Yield: 900 g (90%). Tapped bulk density (B.D.): 0.4 g cm^{-3}. Particle size distribution: d_{10}, 1.5; d_{50}, 3.4; d_{90}, 5.4 µm. BET Surface area: 9 m^2 g^{-1}. TGA (% weight loss): 43.63 (theor. value 43.96%).

Preparation of 'needle-like' aragonite

Aqueous Na_2CO_3 (1 M, 530 g dissolved in 5 L H_2O) and $CaCl_2$ (1 M, 735 g dissolved in 5 L H_2O) were pre-heated to 80 °C. Both the solutions were simultaneously combined in the stainless steel reactor at a feed rate of 90 mL min^{-1}. The temperature of the mixture was maintained at 80 °C till completion of the reaction. The hot slurry (precipitate) was allowed to cool to room temperature, filtered and washed thoroughly with water. The wet cake was then dried overnight at 110 °C and subsequently ground to a fine powder. Yield: 440 g (88%). Tapped bulk density (B.D.): 0.3 g cm^{-3}. Particle size distribution: d_{10}, 5.3; d_{50}, 15.2; d_{90}, 16.4 µm. BET Surface area: 2 m^2 g^{-1}. TGA (% weight loss): 43.78 (theor. value 43.96%).

Instrumentation

The powder X-ray diffraction patterns were recorded on a Siemens D-5000 diffractometer using Cu-Kα ($\lambda = 1.5406$ Å) radiation. The infrared spectra of the ground samples dispersed in KBr pellets were recorded using a Bomem FTIR spectrophotometer (Model: MB 102). High resolution (1 cm^{-1}) FTIR spectra were recorded on self-supported $CaCO_3$ wafers using a Nicolet spectrometer (NICOLET 60SXB). Scanning electron microscopy (SEM) micrographs and Raman spectra of these aragonites were obtained from the Measurement Science Division, Unilever Research Port Sunlight, UK. BET Surface area measurements were carried out on a Quantachrome Autosorb Automated Gas Adsorption System using nitrogen gas as the adsorbate. The average particle size and particle size distribution were obtained on a Malvern MasterSizer machine. The thermogravimetric analyses were carried out on a Perkin-Elmer TGA7 Thermogravimetric Analyzer in the temperature range between 30 and 950 °C.

Results and discussion

Aragonite crystals of unconventional morphologies, like 'cauliflower' and 'flake', were synthesised from equimolar concentrations of aqueous $CaCl_2$ and Na_2CO_3 solutions at ambient conditions (*i.e.*, near room temperature and atmospheric pressure), the only major difference being the absolute concentration (1 M and 2 M) of the reactants. The details of the experimental conditions for the formation of these aragonites are summarised in Table 1. In the case of 'cauliflower-like' aragonite the reaction temperature was determined to be a critical factor in governing the preferential formation of aragonite possessing this morphology. On the other hand, the concentrations of the reactants were found to play a predominant role in the formation of 'flake-like' aragonite at room temperature.

We have investigated the concentration dependence of the reactants in the present reaction *vis-à-vis* the phase and morphology of the final product. When the reaction was performed with higher initial reactant concentrations (*e.g.*, 3 M in both), calcite with rhombohedral morphology was the sole product. Lower reactant concentrations (*e.g.*, 0.5 M in both) resulted in the formation of an intergrowth of calcite and aragonite with rhombohedral/needle-like morphology. Additionally, for the purpose of spectroscopic comparison, an authentic aragonite sample with 'needle-like' morphology was prepared following the literature method.[27]

Characterisation

Aragonite can be distinguished from calcite and vaterite on the basis of its characteristic powder X-ray diffraction (XRD) pattern and vibrational (IR/Raman) spectra. Fig. 2 shows the powder X-ray diffraction patterns of 'cauliflower', 'flake' and 'needle-like' aragonite. Although there are no shifts in peak

Table 1 Experimental conditions for the formation of aragonite samples

Aragonite sample	Reaction temperature/°C	Reactant, concentration[a]	Sequence of addition and feed rate
Flake-like	25	$CaCl_2$, 2 M Na_2CO_3, 2 M	$CaCl_2$ added to Na_2CO_3 at a rate of 90 mL min^{-1}
Cauliflower-like	32	$CaCl_2$, 1 M Na_2CO_3, 1 M	$CaCl_2$ added to Na_2CO_3 at a rate of 90 mL min^{-1}
Needle-like	80	$CaCl_2$, 1 M Na_2CO_3, 1 M	Simultaneous addition of $CaCl_2$ and Na_2CO_3 at a rate of 90 mL min^{-1}

[a] No additive or crystal habit modifier used.

positions, the sharpness and intensities of the XRD lines (width at half-height) differ significantly amongst these three aragonites. Quantitative powder X-ray diffraction experiments were performed in order to assess their relative degrees of crystallinity. The area under the principal XRD line at 3.39 Å (2θ: 26.3°) for the 'flake' and 'cauliflower-like' aragonite samples was found to be ~20% and ~50% of that of the 'needle-shaped' aragonite. In addition to the decrease in intensities, the peak shapes for 'cauliflower' and 'flake-like' aragonite were found to be broadened. This broadening phenomenon is more pronounced in the case of the 'cauliflower-like' aragonite than that of the 'flake-like' aragonite, and is indicative of a lesser degree of crystallinity in these two aragonites than the authentic 'needle-like' aragonite sample.

Aragonite displays a characteristic symmetric carbonate stretching vibration (ν_1) at 1083 cm^{-1} and a carbonate out-of-plane bending vibration (ν_2) at 854 cm^{-1} in its FTIR spectrum. While the symmetric stretching (ν_1) vibration is both infrared and Raman active for aragonite, it is only Raman active in the case of calcite. Thus, the peak at ~1080 cm^{-1} is sometimes used to quantify aragonite from a mixture of aragonite/calcite. On the other hand, the out-of-plane bending (ν_2) vibrational mode is infrared active for all the three polymorphs, but there are some characteristic shifts among these. For calcite and vaterite, the positions of the corresponding ν_2 vibrations are very similar and appear at ~875 cm^{-1}, whereas for aragonite this vibration appears at ~855 cm^{-1}. Characteristic carbonate infrared vibrations for calcite, aragonite and vaterite are shown in Fig. 3.

In the present case, all three aragonite samples exhibited ν_1 and ν_2 bands at 1083 and 854 cm^{-1} respectively in their FTIR spectra. An interesting feature observed in the FTIR spectrum of the 'flake-like' aragonite is that its ν_2 band is shifted to higher energy by ~4 cm^{-1} compared to the 'cauliflower' and 'needle-shaped' aragonite, while the rest of the vibrational bands displayed no shifts (Fig. 4, Table 2). Repeated infrared measurements on two different instruments operating at high resolution (1 cm^{-1}) confirmed this observation of an upward band shift in the ν_2 band of 'flake-like' aragonite to be genuine.

Raman spectra can also be used to fingerprint and distinguish aragonite from the other two calcium carbonate phases. The Raman spectra of all three aragonite samples described in this paper are displayed in Fig. 4B and peak positions are listed in Table 2. The strongest line in each spectrum is the ν_1 symmetric stretch of CO_3^{2-} ion at ~1080 cm^{-1} (not shown in the figure). A pair of peaks at 700 and 704 cm^{-1} is characteristic of aragonite[28] and is present in all three of our samples. For aragonite, the site symmetry of the CO_3^{2-} ion causes the two doubly degenerate ν_4 'in-plane' bending modes to split into a pair of nondegenerate modes.[29] Thus the number of modes expected in both the Raman and infrared spectra of aragonite is six, compared to three in calcite. The splitting of the ν_4 band in all three of our samples ascertained that these were pure aragonites. In addition, the ν_2 vibration is also observed at 852–854 cm^{-1} although the intensity is very weak.

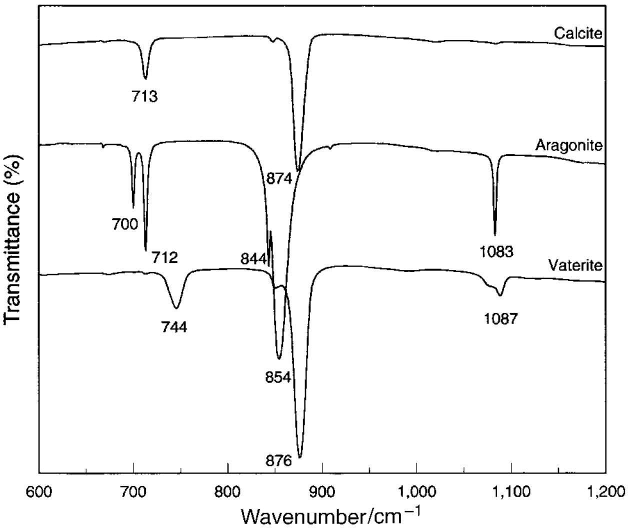

Fig. 3 FTIR spectra of calcite, aragonite and vaterite showing their characteristic carbonate vibrational bands.

Scanning electron microscope (SEM) micrographs of the 'cauliflower', 'flake' and 'needle-like' aragonite samples are shown in Fig. 5. The differences in the topography become evident from their SEM micrographs. There is a discrete and uniform distribution of the agglomerated particles in the 'cauliflower-like' aragonite which is not present in the other two systems. The 'flake-like' aragonite is devoid of any well defined crystallite shape and appears as a cluster of several nanoparticles. Interestingly, these aragonite samples differ in their bulk density properties as well. The 'cauliflower-like' material possesses a very high bulk density and is free flowing in nature, a property which resembles vaterite. On the other hand, the 'needle' and 'flake-like' materials are very fluffy in nature, the latter being slightly heavier than the former. It is unusual to find such a wide variation of morphology and bulk density within aragonitic systems.

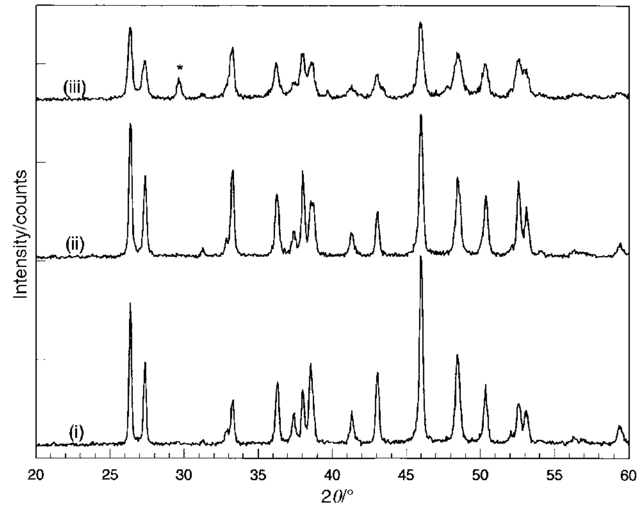

Fig. 2 Powder X-ray diffractograms of (i) 'needle-like', (ii) 'flake-like' and (iii) 'cauliflower-like' aragonites (*: calcite peak).

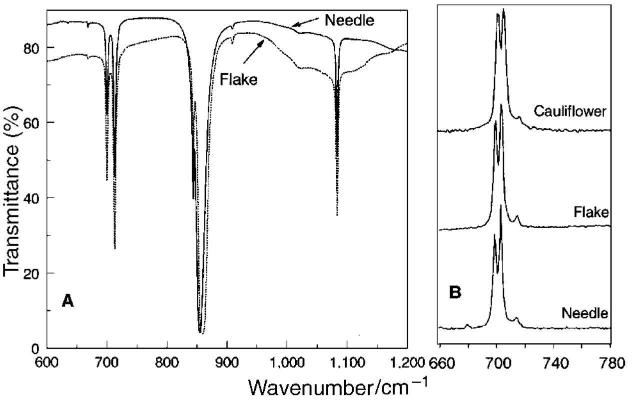

Fig. 4 (A) Segmented FTIR spectra (600–1200 cm^{-1}) of 'flake-like' and 'needle-like' aragonites. (B) Raman spectra showing the characteristic doublet features due to the 'in-plane' bending mode of the carbonate group in all three aragonite samples.

Table 2 Observed vibration frequencies^a (in cm^{-1}) of the carbonate ion in three aragonite samples

Sample	Symmetric stretching (ν_1)/cm^{-1}	Out-of-plane bending (ν_2)/cm^{-1}	Asymmetric stretching (ν_3)/cm^{-1}	In-plane bending (ν_4)/cm^{-1}
Flake-like aragonite	1083 (IR) 1082 (Raman)	858 (IR) 852 (Raman)^a	1483 (IR)	700, 713 (IR) 700, 704 (Raman)
Cauliflower-like aragonite	1082 (IR) 1081 (Raman)	855 (IR) 854 (Raman)^a	1482 (IR)	699, 713 (IR) 702, 706 (Raman)
Needle-like aragonite	1083 (IR) 1081 (Raman)	854 (IR) 852 (Raman)^a	1480 (IR)	700, 712 (IR) 700, 704 (Raman)

^{a}Weak.

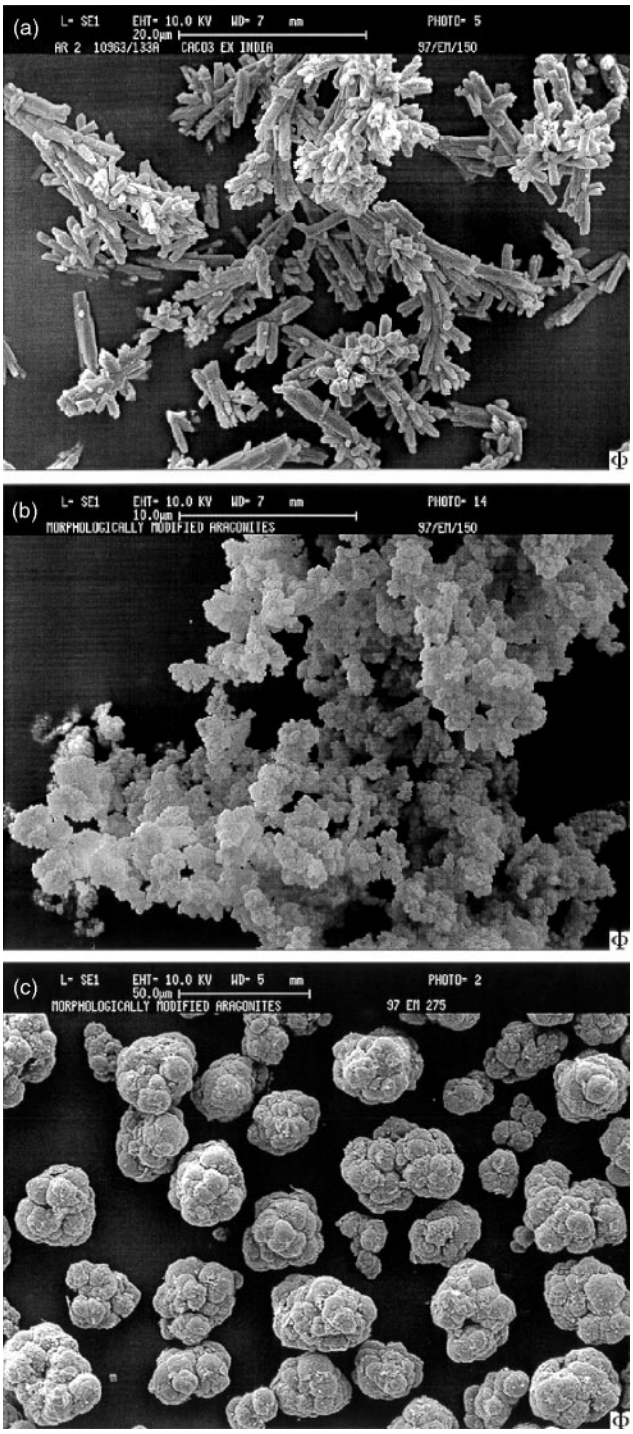

Fig. 5 Scanning electron micrographs of (a) 'needle-like', (b) 'flake-like' and (c) 'cauliflower-like' aragonite samples. Scale bars shown in the SEM pictures are: (a) 20 µm, (b) 10 µm and (c) 50 µm.

Mechanistic insights into the formation of 'cauliflower' and 'flake-like' aragonite

The present study demonstrates that it is possible to prepare aragonitic materials displaying unconventional morphologies by carefully controlling the reaction conditions. Though we do not fully understand the mechanistic implications of the preference of one morphology type over another, we believe that the initial homogeneous nucleation processes play an important role in controlling the final aragonite topography.

In order to gain insights into the mechanism which governs the phase transformation during the course of the reaction leading to the formation of both the 'cauliflower' and 'flake-like' aragonite, aliquots from the reaction mixture were withdrawn at specific time intervals. After rapid filtration, X-ray powder diffraction patterns of the wet calcium carbonate cakes were recorded in order to determine their phase compositions. In the case of 'cauliflower-like' aragonite, the phases present at different time intervals, as summarised in Table 3, were a mixture of calcite and aragonite. The calcitic component gradually decreased with time at the expense of the growth of 'cauliflower-like' aragonite, and at the end of the reaction aragonite was the sole polymorph. In contrast, the phase compositions for 'flake-like' aragonite as monitored during the course of the reaction were a mixture of calcite and vaterite during the early stages of the reaction, with subsequent conversion of vaterite to calcite as the reaction progressed. Interestingly, the phase composition changes to aragonite in a narrow time interval, mid-way through the reaction, subsequent to which this aragonite remains stable till the completion of the reaction. It is evident from the above data that the formation of the 'cauliflower-like' aragonite occurs much earlier during the reaction (as confirmed by SEM), while the same is not true for the formation of the 'flake-like' aragonite. Calcite and vaterite formed during the initial stages of the 'flake-like' aragonite synthesis were found to possess their conventional rhombohedral and spheroidal morphologies, respectively. Thus, the formation of the 'cauliflower' and 'flake-like' aragonite follow different mechanistic pathways. The change in phase composition from calcite to 'flake-like' aragonite within a short time span is very unusual and cannot be explained on the basis of solubility considerations. Solubility products for calcite, aragonite and vaterite at 25 °C are 3.31×10^{-9}, 4.61×10^{-9} and 1.22×10^{-8} M^2 respectively.[30] Thus the dissolution of calcite particles leading to the formation of aragonite is not a thermodynamically feasible process.

At any particular instant during the reaction, the system contains precipitated calcium carbonate (as different crystalline phases and possibly some amorphous phase), a solution of sodium chloride, the concentration of which builds up slowly with the progressive addition of calcium chloride solution to the system, and sodium carbonate solution whose concentration depletes upon such addition. It is difficult to comprehend how progressive changes in these parameters would lead to a drastic change in the phase and morphology of the aragonite polymorph formed. This is more true in the case of the formation of the 'flake-like' aragonite compared to its 'cauliflower' congener. The specificity of the experimental conditions

Table 3 Composition of $CaCO_3$ polymorphs[a] at different time intervals during synthesis

Time/min	'Cauliflower-like' aragonite	'Flake-like' aragonite
5	Calcite (80%) + Aragonite (20%)	Calcite (60%) + Vaterite (40%)
10	Calcite (45%) + Aragonite (55%)	Calcite (80%) + Vaterite (20%)
25	Calcite (15%) + Aragonite (85%)	Calcite (100%)
35	Calcite (10%) + Aragonite (90%)	Calcite (100%)
45	Calcite (6%) + Aragonite (94%)	Aragonite (100%)
60	Calcite (4%) + Aragonite (96%)	Aragonite (100%)

[a]Based on powder X-ray diffraction results.

required for the syntheses of the 'cauliflower' and the 'flake-like' aragonites indicates that there exists a narrow kinetic window within which temperature effects as well as initial reagent concentrations play a key role in governing the preferential formation of aragonite of either of these morphologies.

It can also be reasoned that a possible intergrowth of an amorphous $CaCO_3$ phase along with aragonite during nucleation and the subsequent crystal growth process are responsible for influencing the morphology of the aragonite obtained. During the initial stages of reaction, the formation of a thick gelatinous mass in the case of both 'cauliflower' and 'flake-like' aragonites is a strong indication of the presence of an amorphous calcium carbonate phase which might be key to dictating the final polymorph and morphology. Interestingly, a broad feature at $\sim 1090\ cm^{-1}$ in the FTIR spectra,[9] coupled with a lesser degree of crystallinity from X-ray diffraction studies on these aragonites, suggests the presence of some degree of amorphosity in both the 'cauliflower' and 'flake-like' aragonites in their final form. From the results of the X-ray diffraction studies, it is clear that the 'cauliflower' aragonite is less crystalline than its 'flake-like' aragonitic counterpart.

In the case of aragonite possessing a needle-like morphology, its crystal growth is preferentially expressed along the *c*-axis, relative to the other crystallographic directions. In contrast, it seems that the crystal growth in the 'cauliflower-like' aragonite is almost isotropic thereby leading to the formation of a near spheroidal morphology. Although there are known examples of the presence of spherulitic aragonite clusters in some biogenic materials, this is the first time that a spheroidal aragonite has been prepared under ambient laboratory conditions, using the solution method of synthesis and without employing any additives/crystal habit modifiers. These aragonites are stable at room temperature for long periods, but transform to calcite when heated to 500 °C in air.[31]

Conclusions

Aragonite is usually synthesised with needle-like morphology. This report demonstrates the syntheses of two morphologically modified aragonites by the double decomposition reaction of $CaCl_2$ and Na_2CO_3, under ambient conditions. The two reaction parameters which were found to have the most significant effects on the morphology of the final aragonitic phase are the absolute concentration of reagents and the temperature of the reaction. Both 'cauliflower' and 'flake-like' aragonites are spectroscopically similar to their 'needle-like' congener, except that they are less crystalline in nature and they exhibit minor differences in their FTIR spectra. It is difficult to understand the preferential formation of aragonite with unconventional morphologies at room temperature, however, a plausible mechanism is advanced by investigating the changes in their phase composition during synthesis. While the formation of the 'cauliflower-like' aragonite occurs almost instantly from the commencement of reaction, in the case of the 'flake-like' aragonite an unusual phase transformation from calcite to aragonite was noticed. Formation of amorphous calcium carbonate during the initial stages of the reaction plays a crucial role in governing the phase and morphology of the final products.

Acknowledgements

We thank Drs. Ian Clark and Marilyn Carey of the Measurement Science Division, Unilever Research Port Sunlight Laboratory, UK for providing us with the Raman spectral data and SEM images of various calcium carbonate samples, respectively. Thanks are due to our colleague, Dr. Amitava Pramanik, for helpful discussions.

References

1 H. Lowenstam and S. Weiner, *On Biomineralization*, Oxford University Press, New York, 1989.
2 L. Addadi and S. Weiner, *Angew. Chem., Int. Ed. Engl.*, 1992, **31**, 153.
3 A. Berman, J. Hason, L. Leiserowitz, T. F. Koetzle, S. Weiner and L. Addadi, *Science*, 1993, **259**, 776.
4 S. Weiner and L. Addadi, *J. Mater. Chem.*, 1997, **7**, 689.
5 B. R. Heywood and S. Mann, *Adv. Mater.*, 1994, **6**, 9.
6 S. Mann and G. A. Ozin, *Nature*, 1996, **382**, 313.
7 S. Mann, *J. Mater. Chem.*, 1995, **5**, 935.
8 J. A. H. Oates, *Lime and Limestone: Chemistry and Technology, Production and Uses*, Wiley-VCH, Weinheim, 1998.
9 J. Aizenberg, G. Lambert, L. Addadi and S. Weiner, *Adv. Mater.*, 1996, **8**, 222.
10 L. Merrill and W. A. Bassett, *Acta Crystallogr. Sect. B*, 1975, **31**, 343.
11 L. Addadi, J. Aizenberg, S. Albeck, G. Falini and S. Weiner, *Supramolecular Stereochemistry*, ed. J. S. Siegel, Kluwer Academic Publishers, Netherlands, 1995, pp. 127–139.
12 S. Mann, B. R. Heywood, S. Rajam and J. D. Birchall, *Nature*, 1988, **334**, 692.
13 S. Rajam, B. R. Heywood, J. B. A. Walker, S. Mann, R. J. Davey and J. D. Birchall, *J. Chem. Soc., Faraday Trans.*, 1991, **87**, 727.
14 B. R. Heywood, S. Rajam and S. Mann, *J. Chem. Soc., Faraday Trans.*, 1991, **87**, 735.
15 J. M. Didymus, P. Oliver, S. Mann, A. L. DeVries, P. V. Hauschka and P. Westbroek, *J. Chem. Soc., Faraday Trans.*, 1993, **89**, 2891.
16 S. Mann, D. A. Archibald, J. M. Didymus, T. Douglas, B. R. Heywood, F. C. Meldrum and N. J. Reeves, *Science*, 1993, **261**, 1286.
17 J. M. Didymus, S. Mann, W. J. Benton and I. R. Collins, *Langmuir*, 1995, **11**, 3130.
18 A. L. Litvin, L. A. Samuelson, D. H. Charych, W. Spevak and D. L. Kaplan, *J. Phys. Chem.*, 1995, **99**, 12065.
19 A. L. Litvin, S. Valiyaveettil, D. L. Kaplan and S. Mann, *Adv. Mater.*, 1997, **9**, 124.
20 A. L. Litvin, D. L. Kaplan and C. Sung, *J. Mater. Sci.*, 1997, **32**, 2233.
21 J. Lahiri, G. Xu, D. M. Dabbs, N. Yao, I. A. Aksay and J. T. Groves, *J. Am. Chem. Soc.*, 1996, **119**, 5449.
22 A. Lopez-Macipe, J. Gomez-Moale and R. Rodriguez-Clemente, *J. Cryst. Growth*, 1996, **166**, 1015.
23 J. Kuther and W. Tremel, *Chem. Commun.*, 1997, 2029.
24 S. D. Sims, J. M. Didymus and S. Mann, *J. Chem. Soc., Chem. Commun.*, 1995, 1031.
25 M. M. Reddy and G. H. Nancollas, *J. Colloid Interface Sci.*, 1971, **36**, 166.
26 V. A. Juvekar and M. M. Sharma, *Chem. Eng. Sci.*, 1973, **28**, 825.
27 J. L. Wray and F. Daniels, *J. Am. Chem. Soc.*, 1957, **79**, 2031.
28 G. Behrens, L. T. Kuhn, R. Ubic and A. H. Heuer, *Spectrosc. Lett.*, 1995, **28**, 983.
29 A. Anderson, *Spectrosc. Lett.*, 1996, **29**, 819.
30 L. Brecevic and A. E. Nielsen, *J. Cryst. Growth*, 1989, **98**, 504.
31 D. Chakrabarty and S. Mahapatra, manuscript in preparation.

Paper 9/05407C